Biosensors and Bioelectronics 144 (2019) 111695

Contents lists available at ScienceDirect

Biosensors and Bioelectronics

journal homepage: www.elsevier.com/locate/bios

Biosensors for epigenetic biomarkers detection: A review

Chen-chen Li[1], Zi-yue Wang[1], Li-juan Wang**, Chun-yang Zhang*

College of Chemistry, Chemical Engineering and Materials Science, Collaborative Innovation Center of Functionalized Probes for Chemical Imaging in Universities of Shandong, Key Laboratory of Molecular and Nano Probes, Ministry of Education, Shandong Provincial Key Laboratory of Clean Production of Fine Chemicals, Shandong Normal University, Jinan, 250014, PR China

ARTICLE INFO

Keywords:
Epigenetic inheritance
Noncoding RNA
DNA methylation
Histone modification
Biosensors
Disease biomarker

ABSTRACT

Epigenetic inheritance is a heritable change in gene function independent of alterations in nucleotide sequence. It regulates the normal cellular activities of the organisms by affecting gene expression and transcription, and its abnormal expression may lead to the developmental disorder, senile dementia, and carcinogenesis progression. Thus, epigenetic inheritance is recognized as an important biomarker, and the accurate quantification of epigenetic inheritance is crucial to clinical diagnosis, drug development and cancer treatment. Noncoding RNA, DNA methylation and histone modification are the most common epigenetic biomarkers. The conventional biosensors (e.g., northern blotting, radiometric, mass spectrometry and immunosorbent biosensors) for epigenetic biomarkers assay usually suffer from hazardous radiation, complicated manipulation, and time-consuming procedures. To facilitate the practical applications, some new biosensors including colorimetric, luminescent, Raman scattering spectroscopy, electrochemical and fluorescent biosensors have been developed for the detection of epigenetic biomarkers with simplicity, rapidity, high throughput and high sensitivity. In this review, we summarize the recent advances in epigenetic biomarkers assay. We classify the biosensors into the direct amplification-free and the nucleotide amplification-assisted ones, and describe the principles of various biosensors, and further compare their performance for epigenetic biomarkers detection. Moreover, we discuss the emerging trends and challenges in the future development of epigenetic biomarkers biosensors.

1. Introduction

Epigenetic inheritance is the mitotically or meiotically heritable change in gene expression or cellular phenotype that occurs without changes in Watson Crick base-pairing of DNA (Wolffe and Matzke, 1999). Since Rustem Tchuraev introduced the concept of an 'epigene' in 1975, epigenetic inheritance has been getting more and more attention because it can regulate many cellular processes (e.g., gene and microRNA expression, DNA-protein interactions, transposable element mobility suppression, cellular embryogenesis, and genomic imprinting) of the organisms through controlling gene expression and transcription (Tikhodeyev, 2018). Enormous researches have shown that the abnormal level of epigenetic inheritance in human cells can lead to the occurrences of developmental disorder (Egger et al., 2004), senile dementia (Iwata et al., 2014), and carcinogenesis progression (Portela and Esteller, 2010). Thus, epigenetic inheritance can function as the innovative biomarker for human diseases and provides new opportunities for cancer diagnosis, treatment and prevention (Verma et al., 2004).

The molecular basis of heritable epigenetics has been studied in a variety of organisms, and the systems of epigenetic inheritance mainly focus on three types including noncoding RNA (ncRNA), DNA methylation, and histone modification (Hulshoff et al., 2018). NcRNAs are a class of functional RNA molecules that can be transcribed from genome but cannot be translated into proteins, including two categories: small ncRNAs and long ncRNAs (Wu et al., 2018). Among ncRNAs, microRNAs (miRNAs, more than 1000 being identified) belonging to small ncRNA (Esquela-Kerscher and Slack, 2006) can target more than 30% of human genome (Friedlander et al., 2014; Hu et al., 2018). MiRNAs play essential roles in many physiological processes (e.g., cell development, differentiation, metabolism, and apoptosis) (Amaral et al., 2008), and even act as the tumor suppressors/oncogenes (Lin and Gregory, 2015) (Yanaihara et al., 2006). DNA methylation occurs at the cytosine residues in cytosine/guanine dinucleotide (CpG) islands by transferring a methyl group from S-adenosylmethionine (SAM) to the carbon 5 of cytosine (Stains et al., 2006), with important roles in vital biological activities including gene transcription, X-chromosome inactivation, and

* Corresponding author.
** Corresponding author.
E-mail addresses: wlj-sdnu@foxmail.com (L.-j. Wang), cyzhang@sdnu.edu.cn (C.-y. Zhang).
[1] These authors contributed equally.

https://doi.org/10.1016/j.bios.2019.111695
Received 17 July 2019; Received in revised form 24 August 2019; Accepted 6 September 2019
Available online 11 September 2019
0956-5663/

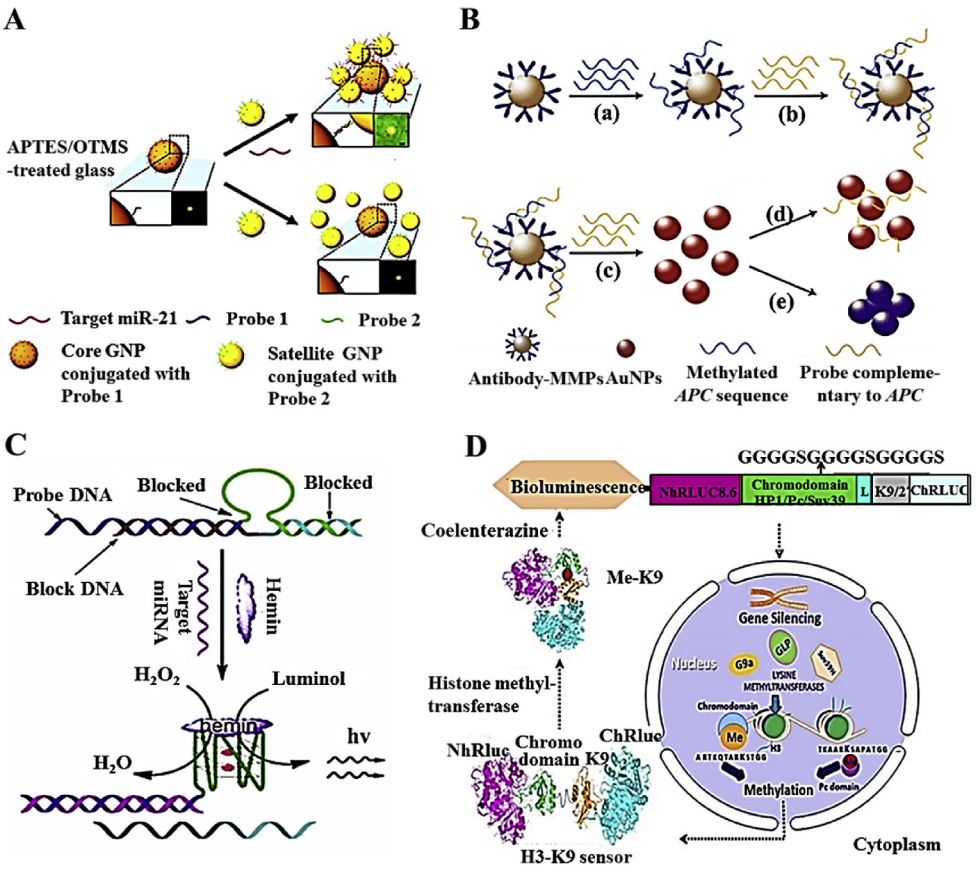

Fig. 1. Development of colorimetric and luminescent biosensors for epigenetic inheritance assays. (A) Schematic illustration of label-free colorimetric detection of miRNA based on the nanoplasmonic core–satellite assembly. The presence of miRNA enables the hybridization of probes 1 with 2, inducing the assembly of core-GNPs and satellite-GNPs and consequently the change of color. Reprinted from (Park and Yeo, 2014) with the permission from the Royal Society of Chemistry. (B) Schematic illustration of colorimetric detection of DNA methylation using MMP and AuNP nanoparticles. Methylated DNAs are captured by anti-5-methylcytosine antibody-conjugated MMPs, inducing the formation of DNA duplexes and consequently the aggregation of AuNPs and the change of color. Reprinted from (Ge et al., 2012) with the permission from the Royal Society of Chemistry. (C) Schematic illustration of luminescent detection of miRNA using both end-blocked peroxidase-mimicking DNAzyme. The presence of miRNA can initiate the strand displacement reaction, inducing the recovery of G-quadruplex structure of DNAzyme for the generation of a chemiluminescence signal. Reprinted from (Li et al., 2017b) with the permission from the American Chemical Society. (D) Schematic illustration of luminescent detection of histones based on the split-enzyme complementation strategy. Methylated K9/K27 can bind with Suv39H1/Pc2 domain to bring two halves of split-RLuc together for the generation of a bioluminescence signal. Reprinted from (Sekar et al., 2015) with the permission from the American Chemical Society. (For interpretation of the references to color in this figure legend, the reader is referred to the Web version of this article.)

pluripotent state maintenance (Lister et al., 2009). Aberrant DNA methylation patterns are closely related to various genetic diseases and cancers (Jones and Baylin, 2002). Histones are a kind of basic structural proteins in eukaryotic chromosomes, and they usually suffer from dynamic reversible posttranslational modifications (e.g., methylation, acetylation, phosphorylation, ubiquitylation, and SUMOylation) at the free amino termini (Bhaumik et al., 2007; Bird, 2007; Shi et al., 2005). Histone-modifying enzymes (HMEs) are responsible for the modifications of histones (Bhaumik et al., 2007), and the dysfunction of histone-modifying enzymes may cause the dysregulation of cell proliferation and tissue development, resulting in developmental defects and various diseases (Ma et al., 2016). Therefore, as both hallmarks of epigenetic inheritance and biomarkers of multiple diseases, the accurate detection of ncRNAs, DNA methylation, histone modifications and HMEs are not only of importance to epigenetics-related biochemical research, but also of significance to diagnosis, prognosis, and therapy of cancers.

Conventional biosensors for epigenetic biomarkers detection mainly include northern blotting (Lagos-Quintana et al., 2001), radiometric assay (Horiuchi et al., 2013; Li et al., 2013), mass spectrometry (MS) (Bonaldi et al., 2004; Li et al., 2012), and immunosorbent assay (Ghadiali et al., 2011; Wynne Aherne et al., 2002). Northern blotting is regarded as a standard method for microRNA assay, but it suffers from poor sensitivity (above nmol), time-consuming steps, and large sample consumption, unsuitable for the low-abundance microRNA assay (Lagos-Quintana et al., 2001). Radiometric assay is the typical method for sensitive detection of microRNA and HMEs, whereas the involvement of radioactive materials limits its widespread applications (Horiuchi et al., 2013; Li et al., 2013). Alternatively, MS can provide a straightforward approach for the quantification of DNA methylation and HMEs, but it involves expensive instruments, complicated sample preparations, and cannot directly detect the targets in complex samples (Bonaldi et al., 2004; Li et al., 2012). Immunosorbent assay utilizes specific antibodies to sense histone modifications generated from a HME reaction (Ghadiali et al., 2011; Wynne Aherne et al., 2002), inevitably involving costly antibodies, stringent conditions, and labour-consuming operations. Recently, some new biosensors including colorimetric (Li et al., 2016; Park and Yeo, 2014; Su et al., 2015; Zhen et al., 2012), luminescent (Chen and Li, 2014; Deng et al., 2013; Hiraoka et al., 2012; Li et al., 2017b; Yoshida et al. 2013, 2016), Raman scattering spectroscopy (Bai et al., 2013; Wang et al., 2015, 2016; Ye et al., 2014; Zhou et al., 2017) electrochemical (Bo et al., 2018; Castaneda et al., 2017; Chen et al., 2017; Ge et al., 2014; Hu et al., 2015; Povedano et al., 2018) and fluorescent assays (Cao and Zhang, 2012; Gilboa et al., 2016; Hu et al., 2018; Ma et al., 2016; Sun et al., 2018; Tang et al., 2018; Wang et al., 2018b; Wen et al., 2013; Zhang and Zhang, 2012; Zhu et al., 2014) have been developed for specific and sensitive detection of epigenetic biomarkers with simplicity, rapidity, and high throughput. In this review, we summarize the recent advances in the development of biosensors for epigenetic biomarkers detection, and classify these biosensors into two categories including the direct amplification-free and the nucleotide amplification-assisted biosensors. Furthermore, we discuss the emerging trends and challenges in the development of biosensors for monitoring epigenetic biomarkers.

2. Direct amplification-free biosensors

The direct amplification-free biosensors are much simpler and rapider than the amplification-assisted biosensors. They do not involve any nucleotide-based amplification and can be applied directly for epigenetic biomarkers detection. Based on different signal transductions, the direct biosensors can be divided into colorimetric, luminescent, Raman scattering spectroscopic, electrochemical and fluorescent

biosensors.

2.1. Colorimetric biosensors

The colorimetric biosensors have the advantages of simplicity, rapidity and cost-effectiveness, and they enable the signal being read out with color changes or even directly monitored via the naked eyes. Specially, owing to high extinction coefficients, strong photostability and excellent biocompatibility of gold nanoparticles (AuNPs), the AuNP-based colorimetric biosensors have attracted enormous interest from researchers (Lee et al., 2007; Li et al., 2017a; Medley et al., 2008; Qu et al., 2011; Shen et al., 2018; Xu et al., 2009). Based on the assembly of gold nanoplasmonic particles (GNPs) into a core-satellite configuration, Yeo et al. reported an on-chip colorimetric biosensor for miRNA detection (Fig. 1A) (Park and Yeo, 2014). Core-GNPs are initially anchored on the 3-aminopropyltriethoxysilane (APTES)/octadecyltrimethoxysilane (OTMS)-treated glass slide, followed by being functionalized with probe 1 and probe 2 to form the satellite-GNPs. In the presence of target miRNA, it can partly hybridize with both probes 1 and 2 to direct the assembly of core-GNPs and satellite-GNPs to form a core-satellite nanostructure, resulting in the color and spectrum changes. This biosensor can measure miRNA with a detection limit of 1 pM and a dynamic range of 10 orders of magnitude, and it exhibits good selectivity towards target miRNA, providing a reliable platform for clinical point-of-care diagnosis.

Based on the magnetic microspheres (MMPs) enrichment and the observation of the color change of GNPs solution, Zeng and colleagues developed a simple biosensor for the detection of methylated DNA (Fig. 1B) (Ge et al., 2012). Methylated substrates are captured and enriched by anti-5-methylcytosine monoclonal antibodies which are conjugated on the MMPs. The subsequent addition of the probes complementary to the methylated substrates results in the formation of DNA duplexes. The probes captured by the microspheres can be released by heat denaturation. Upon the addition of AuNPs, the released probes can induce the aggregation of AuNPs, leading to the color change from purple to red. This biosensor does not require any chemical treatment or enzyme digestion, and it can be used for semi-quantitative analysis of methylated DNA sequences with a detection limit of 80 fmol.

Recently, through assembling the peptide-decorated AuNPs into the network structures, Jiang et al. presented a colorimetric biosensor for multiple HMEs detection (Zhen et al., 2012). HMEs can modify the substrate peptides that are assembled on the AuNPs, which subsequently bind with the divalent immunoglobin G antibody to trigger a network-like assembly of peptide-modified AuNPs, inducing a variation in the plasmon resonance absorption peak accompanied by a visualized color change. This biosensor is highly specific due to the introduction of antibody-based recognition system, and the detection limit is estimated to be 0.2 nM for histone methyltransferase and 0.5 nM for histone acetyltransferase (HAT), respectively.

2.2. Luminescent biosensors

The reported AuNP-based colorimetric biosensors are generally not sensitive enough. In contrast, the luminescent biosensors have a significant improvement in the sensitivity, suitable for a wider range of practical applications. Luminescence is an optical radiation phenomenon produced by a chemical reaction in which chemically excited molecules decay to the ground state, and it can be utilized for the detection of small amounts of analytes via measuring the light emitted by biouminescent or chemiluminescent reactions (Roda et al., 1996; Van de Bittner et al., 2010). Recently, luminescent biosensors have been widely used for the detection of DNAs (Zou et al., 2019), RNAs (Liao et al., 2018), and proteins (Li et al., 2018). Taking advantage of DNAzyme-catalyzed chemiluminescence (Deng et al., 2013), Zhang et al. designed a peroxidase-mimicking DNAzyme whose ends were fixed with block DNA for miRNA assay (Fig. 1C) (Li et al., 2017b). In the presence of target miRNA, the strand displacement reaction between miRNA and the block DNA is initiated, resulting in the recovery of G-quadruplex structure of DNAzyme for the generation of a strong chemiluminescence signal. This biosensor can detect subpicomolar miRNA (the detection limit is 25 pM) without any labeling. It can distinguish single-base mismatch miRNA and quantify miRNA in the complicated samples (e.g., human serum).

Bioluminescence resonance energy transfer (BRET) is a radioactive transmission between the bioluminescent energy donor and the appropriate acceptor (Yu et al., 2016). By using methyl-CpG binding domain (MBD)-fused luciferase, Isao Karube et al. developed a BRET-based biosensor for the measurement of global DNA methylation level (Yoshida et al., 2016). The MBD-luciferase can recognize the methylated sequence, leading to the occurrence of BRET between luciferase and fluorescent DNA-intercalating dye in target DNA. This biosensor can simply detect the global methylation level of plasmid DNA and human genomic DNA with a detection limit of 0.48 μM and 93 nM, respectively.

By taking advantage of the BRET principle, Paulmurugan et al. constructed a genetically encoded molecular biosensor using the split-enzyme complementation to monitor the methylation which occurs at specific locations in N-terminal tail of histones (K9 and K27) (Fig. 1D) (Sekar et al., 2015). When the methylated K9/K27 binds with the Suv39H1/Pc2 domain to bring two halves of split-RLuc together, the biosensor is activated for the generation of a bioluminescence signal that can be imaged in vitro and in vivo. This biosensor can be used for in vivo imaging of lysines 9 and 27 methylation marks of histones (K9 and K27) in different cancer cells (e.g., human embryonic kidney cell line (HEK293T cells), human hepatocellular liver carcinoma cell line (HepG2 cells), and human cervical carcinoma cell line (HeLa cells)), and further applied for in vitro screening and in vivo characterization of new histone methyltransferase inhibitors, holding great potential in epigenetic therapies development.

2.3. Raman scattering spectroscopic biosensors

Due to the limited types of luminescent materials, the luminescent biosensors are not suitable for the multiplexed analysis. In contrast, SERS has distinct advantages of resistance to photo-bleaching and narrow widths of vibrational Raman bands, suitable for the simultaneous detection (Tong et al., 2018). Surface-enhanced Raman scattering (SERS) is a vibrational spectroscopic technique that measures the enhanced Raman intensity of target molecule upon its interaction with the SERS-active nanostructures (Wang et al., 2017). Jiang and colleagues reported a SERS-based biosensor for the detection of histone demethylase activity with the lysine-specific demethylase 1 (LSD1) as a model (Wang et al., 2013). In the presence of LSD1, it can catalyze the demethylation reaction at the special site of peptide to produce the byproduct formaldehyde. With the addition of fomaldehyde-selective probe Purpald, the adduct reaction takes place. Subsequently, the Purpald–formaldehyde adducts can self-assemble on the surface of the peptide-stabilized AuNPs to produce a strong SERS signal. This biosensor exhibits a detection limit of 0.6 nM, and it can be further used to screen potential inhibitors, holding great potential for a wide range of demethylation studies.

To increase the throughput, Ye et al. synthesized three different Raman dye-coded Au nanoparticles with narrow intra-nanogap structures (Au-RNNPs), and developed a SERS-based biosensor for simultaneous detection of multiple miRNAs on the basis of sandwich hybridization (Fig. 2A) (Zhou et al., 2017). The Raman dye-coded Au-RNNPs are initially functionalized with the complementary sequences of target miRNAs to form the SERS nanoprobes. Furthermore, three capture DNAs are designed, which can be coassembled on the micrometer-sized hollow silver microspheres (Ag-HMSs). Three target miRNAs can sandwich hybridize with the corresponding capture probes

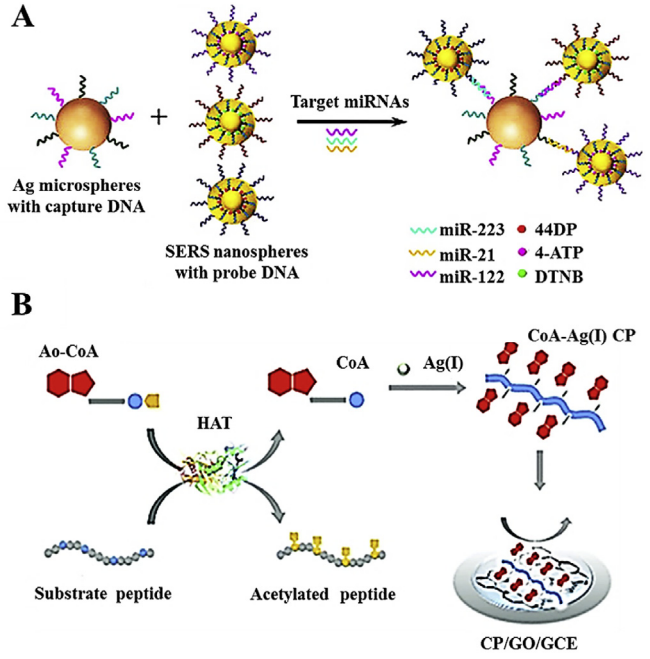

Fig. 2. Development of Raman scattering spectroscopic and electrochemical biosensors for epigenetic inheritance assay. (A) Schematic illustration of SERS-based biosensor for simultaneous detection of multiple miRNAs. The miRNAs can hybridize with the corresponding capture probes and SERS nanoprobes to form three different sandwich complexes, enabling simultaneous detection of three miRNAs. Reprinted from (Zhou et al., 2017) with the permission from the American Chemical Society. (B) Construction of a label-free electrochemical biosensor for the detection of HAT. The presence of HAT induces the generation of CoA-Ag (I) CP which can bind GO to yield an enhanced electrochemical signal. Reprinted from (Hu et al., 2015) with the permission from the Royal Society of Chemistry.

and SERS nanoprobes which have unique SERS spectra, enabling simultaneous detection of three miRNAs in a single sample. This biosensor exhibits a detection limit of 10 fM, and it can be applied for simultaneous detection of three miRNAs in human hepatocellular carcinoma cells, providing a new platform for multiplexed detection of cancer biomarkers.

Recently, by using the embedded-internal SERS nanotags, Matt Trau et al. developed a SERS-based biosensor to simultaneously monitor DNA methylation level and quantify the amount of input genomic DNA (gDNA) (Wang et al., 2016). In this assay, gDNA is enzymatically digested into DNA fragments, and then the biotin-dNTPs are polymerized into the ends of DNA fragments, followed by the incubation with streptavidin-magnetic beads and SERS nanotags to capture and quantify the available biotinylated DNA. Meanwhile, the SERS nanotag-labeled MBD proteins are added to specifically bind the methyl groups in DNA for the quantification of DNA methylation level. This biosensor can detect as low as 0.2 ng of input DNA, and it can differentiate 6.25% changes in DNA methylation. Moreover, it can be used to evaluate the DNA methylation level in both human cancer cells and breast biopsy samples, and even differentiate cells before and after demethylating drug-treatment and distinguish tumor from normal biopsies.

2.4. Electrochemical biosensors

The electrochemical biosensors are developed based on biorecognition and electrochemical transducer which mediate the generation of a measurable electrical signal (Thevenot et al., 2001). In comparison with the SERS-based methods, the electrochemical biosensors have the advantages of simplicity, rapidity, and low cost (Labib et al., 2016). Taking advantage of the unique electrocatalytic activity of the Coenzyme A-silver ion coordination polymer (CoA-Ag (I) CP), Yao et al. developed a label-free electrochemical biosensor for HAT detection (Fig. 2B) (Hu et al., 2015). HAT can catalyze the transfer of acetyl group from acetyl-coenzyme A (Ac-CoA) to lysine residue of substrate peptide, producing e-N-acetyl lysine residue and CoA. The CoA and Ag (I) can yield a novel nucleic acid-mimicking CoA-Ag (I) CP through the in-situ synthesis of a chain-like structure with (-CoA-Ag (I)-) repeated units and multiple adenine bases as the side groups along the polymer backbone. The resultant CoA-Ag (I) CP can bind GO, inducing the remarkably enhanced electrocatalysis towards H_2O_2 reduction. A good linear relationship is obtained between the enhanced current response and the HAT concentration in the range from 0.1 to 100 nM, and the detection limit can reach 0.067 nM. Moreover, this biosensor can be used to assess the HAT inhibitors, proving the great potential of functional CPs in biosensing and drug development.

Inspired by above nucleic acid-mimicking CoA-Ag (I) CP, Dong et al. developed an electrochemical biosensor for miRNA assay by using the oligonucleotide-encapsulated silver nanoclusters (Ag–NCs) as the signal probes (Dong et al., 2012). They designed a molecular beacon (MB) probe and a functional oligonucleotide probe. The MB probes are immobilized on the gold electrode (GE) surface. The functional oligonucleotide probes contain the recognition sequence for hybridization and the template sequence for in situ synthesis of Ag–NCs. In the presence of target miRNA, it hybridizes with the MB probe and the functional probe to form a sandwiched hybrid, bringing the oligonucleotide-encapsulated Ag–NCs close to the electrode surface for the generation of a detectable signal. This biosensor exhibits a detection limit of 67 fM, and it has a linear range of 5 orders of magnitude from 100 fM to 10 nM, providing a promising detection platform for genetic analysis.

To improve sensitivity, Huang et al. took advantage of the specificity of anti-5-methylcytosine antibody towards the methylated cytosine after binding of graphene oxide (GO), and developed an electrochemical DNA biosensor for sensitive quantification of DNA methylation and multiple methylated sites (Huang et al., 2019). GO is modified with anti-5-methylcytosine antibody which can specifically bind with the CpG methylation sites. The horseradish peroxidase (HRP)-labeled IgG secondary antibody can specifically bind the anti-5-methylcytosine antibody and catalyze the oxidation of hydroquinone into benzoquinone in the presence of H_2O_2, generating an electrochemical reduction signal. This biosensor can quantify DNA methylation with a detection limit of 1 fM and a wide linear range of 7 orders of magnitude between 10^{-15} and 10^{-8} M. Moreover, this biosensor exhibits high specificity, good stability and repeatability.

2.5. Fluorescent biosensors

Fluorescence is a phenomenon of light emission upon a molecule absorbing electromagnetic energy (Prolo et al., 2018). Fluorescent biosensors are based on the measurement of fluorescence intensity, and they have been widely applied for the detection of various biomarkers due to their distinct advantages of simple operation and easy readout (Wang et al., 2018a). Liu et al. developed a Förster resonance energy transfer (FRET)-based fluorescent biosensor for simultaneous detection of multiple miRNAs using a single excitation wavelength (Liu et al., 2017). This assay involves a nucleic acid stain TOTO-1 and three fluorescent dyes (i.e., Cy3, Cy3.5, and Cy5) for oligonucleotide labeling, which emit no fluorescence in the absence of target miRNAs. In contrast, target miRNAs can hybridize with the auxiliary probe and the fluorescent dye-labeled oligonucleotides to form the duplexes, intercalating TOTO-1 and fluorescent dyes (i.e., Cy3, Cy3.5, and Cy5) into the duplexes and consequently inducing efficient FRET among them. After spectra crosstalk correction, each miRNA in plasma can be accurately quantified in the presence of other two miRNAs no matter at high or low concentrations. This biosensor can simultaneously quantify three miRNAs with a detection limit of 0.02 nM, and detect miRNAs in human plasma samples, with potential applications in clinical

diagnosis, prognosis, and therapeutic monitoring of early-stage lung cancer.

By integrating the antibody-based fluorescent labeling with single-molecule imaging, Zhang et al. developed a fluorescent biosensor for simultaneous detection of HAT GcN5 and histone methyltransferase (HMT) G9a (Ma et al., 2016). GcN5 can acetylate H3 protein predominantly at lysine residues 14 (K14) and possesses activity towards K9 and K18 (Grant et al., 1999), while G9a is able to catalyze the methylation of H3–K9 and H3–K27 (Tachibana et al., 2001). A peptide substrate containing a biotinylated N-terminal and the recognition sites of GcN5 and G9a is designed. GcN5 and G9a can transfer the acetyl and the methyl groups to peptide substrates, respectively, making the peptides bound by Alexa Fluor 488-conjugated anti-acetyl lysine and Alexa Fluor 647-conjugated anti-methyl lysine. With the addition of streptavidin-coated magnetic beads, the dye-labeled peptides are captured, separated and eluted. Eventually, the released fluorophores from the peptides can be simply counted by total internal reflection fluorescence (TIRF)-based single-molecule imaging. This biosensor exhibits a detection limit of 21 pM for GcN5 and 12 pM for G9a, and it can be used for the screening of inhibitors and the quantification of histone-modifying enzymes even in crude cell extracts, providing a new approach to study complex biological processes regulated by multiple HMEs.

3. Nucleotide amplification-assisted biosensors

Despite the wide applications of direct biosensors, they inevitably suffer from relatively poor sensitivity. To improve the detection sensitivity, the amplification approaches have been introduced for epigenetic biomarkers analysis. In this section, we focus on the frequently used nucleotide amplification-based strategies including PCR, strand displacement amplification, exonuclease-/endonuclease-assisted signal amplification, and ligase chain reaction for ncRNAs, DNA methylation, histone modifications, and HMEs assays.

3.1. PCR amplification

PCR is a thermal cycle-based DNA amplification technique with the requirement of a stringent primer/template design and precise thermal cycling, and it can amplify a very small amount of DNA in the picograms range and even in the presence of diverse contaminants (Cenis, 1992). Gong et al. developed a template repairing-PCR (TR-PCR) technology for sensitive miRNA detection based on miRNA-primed bypass synthesis at the abasic sites of template (Fig. 3A) (Zhou et al., 2019). They designed a damaged PCR template containing one tetrahydrofuran site. The annealing of target miRNA with the DNA template induces the DNA replication. Klenow fragment DNA polymerase can catalyze the translesional synthesis at the tetrahydrofuran site, resulting in the generation of a new template complementary to the damaged DNA template. In the absence of miRNA, the damaged template cannot be repaired, and the tetrahydrofuran site in the damaged template may block the DNA synthesis. The TR-PCR can avoid the complicated design of reverse transcription primers from short lengths of miRNA, greatly simplifying the operation procedures. This TR-PCR-based biosensor can achieve a detection limit of as low as 2 amol. It can discriminate the mismatched miRNAs and measure miRNAs in real samples (i.e., mice liver tissues).

With the assistance of PCR amplification technique, Kazunori Ikebukuro et al. constructed a fluorescent biosensor for sensitive detection of DNA methylation level (Fig. 3B) (Hiraoka et al., 2012). The methylated DNA with a zinc-finger recognition site is precipitated by methyl CpG-binding domain (MBD) protein that is immobilized on the glutathione-coated magnetic beads via GST. Then MBD protein is eluted by heating, and the target DNA is amplified via PCR using the biotinylated primers. The obtained products are immobilized on the streptavidin-coated magnetic beads and subsequently detected by using

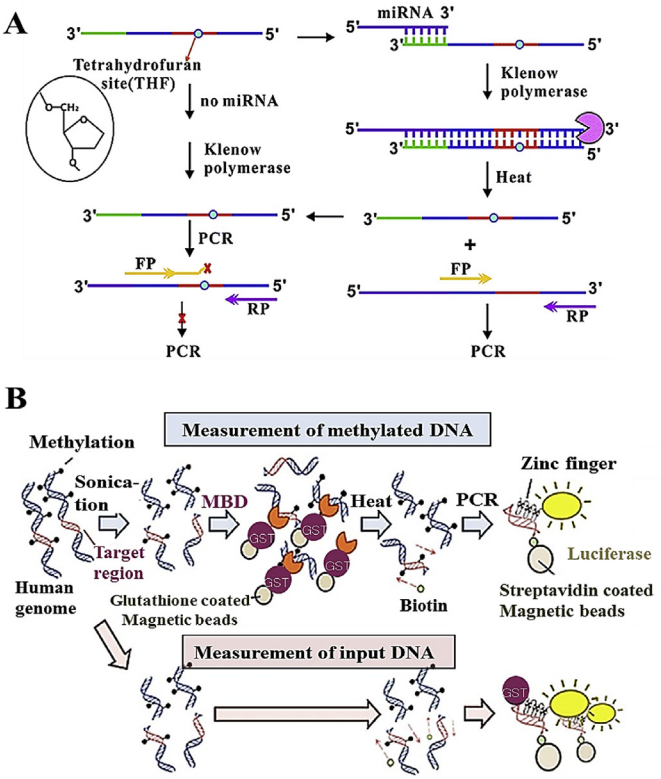

Fig. 3. Development of PCR-based biosensors for epigenetic inheritance assay. (A) Schematic illustration of real-time detection of miRNA based on DNA template-repairing at tetrahydrofuran sites. The annealing of miRNA with the damaged PCR template induces the translesional synthesis at tetrahydrofuran sites, resulting in an enhanced fluorescent signal. Reprinted from (Zhou et al., 2019) with the permission from the Royal Society of Chemistry. (B) Schematic illustration of fluorescent detection of DNA methylation using MBD protein and luciferase-fused ZF protein. Methylated DNA is amplified by PCR using the biotinylated primers, and the obtained products are detected by using luciferase-fused ZF protein. Reprinted from (Hiraoka et al., 2012) with the permission from the American Chemical Society.

luciferase-fused zinc finger protein. This biosensor can detect the methylation level even from 3.3×10^2 copies of human genomic DNA, and quantify the methylation level of androgen receptor gene promoter region in human prostate cancer cell lines (i.e., LNCaP cells, PC3 cells, and Du145 cells) and whole blood cells without the involvement of bisulfite treatment.

Kazunori Ikebukuro et al. further developed a PCR-based biosensor for the detection of histone modification through chromatin immunoprecipitation in combination with zinc finger luciferase-based BRET (ChIP-ZF-BRET) (Yoshida et al., 2013). Histone modification antibodies are used to perform ChIP, and the target region containing the zinc finger recognition site can be amplified by PCR using the biotinylated primers. The obtained products are immobilized on the magnetic beads and subsequently quantified by BRET between the zinc finger protein-fused luciferase (donor) and the DNA intercalating dye (receptor). Owing to the introduction of ChIP-ZF-BRET system, this biosensor exhibits a detection limit of 10 copies, and it can detect histone modification at the androgen receptor gene promoter region in human prostate cancer cell lines (i.e., LNCaP cells and Du145 cells), suitable for simultaneous detection of histone modification and DNA methylation in clinical diagnoses.

3.2. Strand displacement amplification

To avoid precise thermal cycling of PCR, strand displacement amplification (SDA, an isothermal DNA amplification technique) is

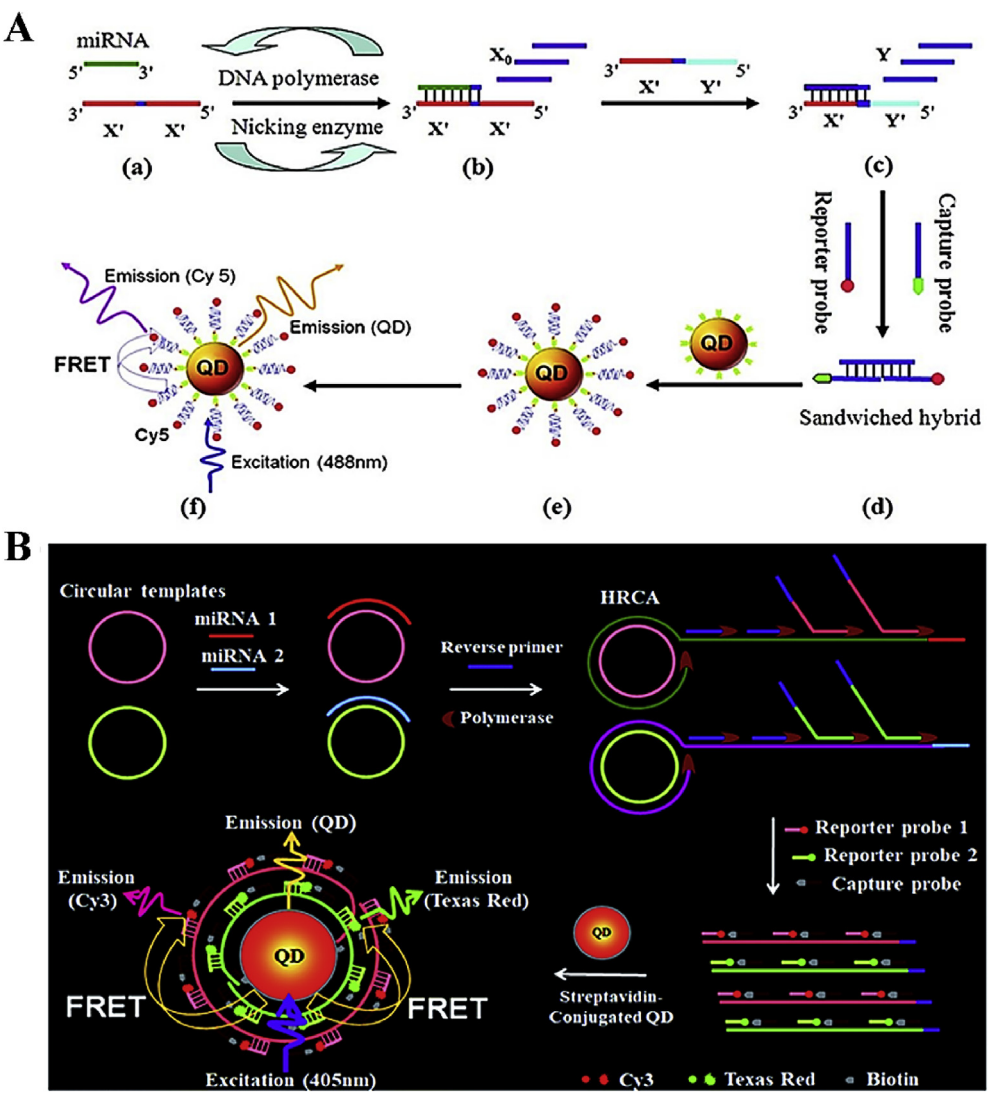

Fig. 4. Development of SDA-based biosensors for epigenetic inheritance assay. (A) Schematic illustration of fluorescent detection of miRNA using a two-stage EXPAR. The presence of miRNA induces EXPAR to produce the reporter oligonucleotides which subsequently hybridize with the biotinylated capture probes and the Cy5-labeled reporter probes to form the sandwich hybrids, resulting in efficient FRET between the QD and Cy5. Reprinted from (Zhang and Zhang, 2012) with the permission from the American Chemical Society. (B) Schematic illustration of simultaneous detection of multiple miRNAs by integrating isothermal amplification with the QD-based FRET. The miR-21 and miR-221 specifically hybridize with two circular templates to initiate HRCA, and then the resultant products hybridize with the biotinylated capture probes and the Cy3-/Texas red-labeled reporter probes to form the sandwich hybrids, respectively, inducing efficient FRET between the QD and Cy3/Texas red. Reprinted from (Hu et al., 2018) with the permission from the Royal Society of Chemistry. (For interpretation of the references to color in this figure legend, the reader is referred to the Web version of this article.)

developed. SDA is driven by the primer extension polymerization to generate abundant target sequences of interest (Van Ness et al., 2003). Based on nicking endonuclease-mediated circular SDA, Zhang et al. developed an exponential amplification reaction (EXPAR)-based SERS biosensor for simultaneous detection of multiple miRNAs (Ye et al., 2014). This biosensor involves a linear amplification for the conversion of target miRNA to the single-stranded triggers and a circular exponential amplification for the generation of abundant triggers. The resultant triggers can be hybridized with a reporter probe and an AuNP-modified capture probe to form a sandwich complex, enabling the assembly of large amounts of reporter probes on the surface of AuNPs and consequently the generation of an enhanced SERS signal. This biosensor displays a detection limit of 0.5 fM, and it can distinguish the perfect matched miRNAs from one-base mismatched ones. Moreover, it exhibits good performance in real sample (e.g., lung cancer cells) analysis. Furthermore, Zhang et al. developed a single-quantum-dot-based nanosensor for miRNA assay based on a two-stage EXPAR (Fig. 4A) (Zhang and Zhang, 2012). The two-stage EXPAR can convert target miRNA to a large number of reporter oligonucleotides which can hybridize with the biotinylated capture probes and the Cy5-labeled reporter probes to form the sandwich hybrids. The resultant sandwich hybrids can assemble on the surface of quantum dot (QD) to induce FRET from the QD to Cy5. This biosensor is ultrasensitive with a detection limit of 0.1 aM, and it can discriminate single-nucleotide differences among miRNA family members. Recently, Zhang et al. demonstrated the simultaneous detection of multiple miRNAs by integrating hyperbranched rolling cycle amplification (HRCA) with the QD-based FRET (Fig. 4B) (Hu et al., 2018). Two circular templates are designed to specifically hybridize with miR-21 and miR-221, respectively, for the initiation of HRCA reactions. The resultant products can hybridize with the biotinylated capture probes and the Cy3-/Texas red-labeled reporter probes to form the sandwich hybrids which can assemble on the QD surface to induce efficient FRET between the QD and Cy3/Texas red. This biosensor exhibits good specificity and high sensitivity with a detection limit of 7.2×10^{-16} M for miR-21 and 1.6×10^{-17} M for miR-221, and it can be applied for simultaneous detection of multiple miRNAs in human lung adenocarcinoma cell line (A549 cells).

Furthermore, Zhang et al. developed a label-free biosensor for methylation status detection in specific CpG sites based on ligation-mediated hyperbranched rolling circle amplification (HRCA) (Cao and Zhang, 2012). After bisulfite treatment of methylated target DNA, the linear padlock probe can be circularized, and the resultant product may serve as a template for HRCA. The amplification product can be quantified by using fluorescent dye SYBR Green I as the stainer. This biosensor exhibits high sensitivity with a detection limit of 0.8 fM, and it can distinguish 0.01% methylation level from the mixture. Moreover, this biosensor can measure methylation level in human lung cancer cell lines with a detection limit of 2 ng. Very recently, Li et al. reported a highly specific and sensitive biosensor for DNA methylation detection

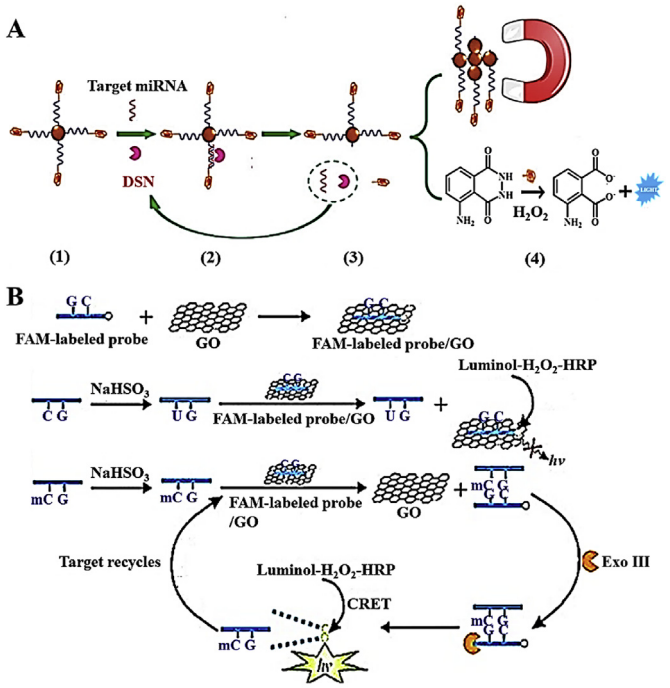

Fig. 5. Development of EASA-based biosensors for epigenetic inheritance assay. (A) Schematic illustration of chemiluminescent detection of miRNA based on DSN-induced DNAzymes. The presence of miRNA induces DSN-assisted cyclic release of DNAzymes from magnetic beads, generating an amplified chemiluminescence signal. Reprinted from (Deng et al., 2013) with the permission from the Royal Society of Chemistry. (B) Schematic illustration of site-specific detection of DNA methylation on the basis of Exo III-mediated recycling amplification. The presence of methylated DNA can induce the cyclic release of FAM-labeled probes from GO, resulting in CRET from luminol–H_2O_2–HRP to FAM. Reprinted from (Chen and Li, 2014) with the permission from the Elsevier.

by using a methylation-dependent restriction endonuclease GlaI in combination with EXPAR (Sun et al., 2018). The treatment of target DNA with GlaI induces the specific cleavage of methylated cytosines, generating the new end fragments which can act as the primers to trigger EXPAR. The amplification products can be simply detected by using SYBR Green I as the fluorescent indicator. The detection limit is pushed down to 200 aM. Importantly, this biosensor can identify as low as 0.01% methylated DNA in the presence of excess unmethylated DNA, and detect site-specific DNA methylations in real genomic DNA extracted from human colon cell line (HCT116 cells).

3.3. Exonuclease-/endonuclease-assisted signal amplification

Exonuclease-/endonuclease-assisted signal amplification (EASA) takes advantages of either exonuclease or endonuclease to cyclically digest/cleave the specific nucleotide sequences for the achievement of signal amplification. By taking advantage of the unique enzymatic activity of duplex-specific nuclease (DSN), Gao et al. designed a biosensing probe for sensitive detection of miRNA (Fig. 5A) (Deng et al., 2013). This biosensing probe contains a miRNA capturing segment and a DNAzyme sequence, and it is assembled on the surface of magnetic bead. When the biosensing probe hybridizes with target miRNA, its miRNA capturing segment can be cleaved by DSN, inducing the dissociation of DNAzyme moiety from the magnetic bead and the release of miRNA strands. Especially, DSN may induce the cyclic digestion of miRNA capturing segments to release a large number of DNAzyme moieties which can generate an enhanced chemiluminescence signal in the presence of luminol and H_2O_2. This biosensing probe exhibits a detection limit of 10 fM, and it can even discriminate the single-base mismatch. Recently, Zhang et al. developed a quencher-free fluorescent biosensor for miRNA detection using a 2-aminopurine probe in combination with endonuclease (Nb.BtsI) and lambda exonuclease (Zhu et al., 2014). The 2-aminopurine has a weak fluorescence signal when being incorporated into DNA strands, but the fluorescence intensity highly enhances when being free. The 2-aminopurine probe can hybridize with a short helper DNA to reduce the background signal. The binding of target miRNAs with the 2-aminopurine probe may initiate the extension reaction and replace the helper DNA. The resultant DNA duplexes are cyclically digested by nicking enzyme and lambda exonuclease, releasing the extended targets and the free 2-aminopurine molecules for significant fluorescence enhancement. The detection limit can reach 0.3 fmol. This biosensor can discriminate the single-base difference among miRNA family members, and distinguish the expression of miRNAs in lung tissues between the non-small cell lung cancer patients and the healthy persons.

In addition, Li et al. developed a chemiluminescence resonance energy transfer (CRET) biosensing platform for the detection of site-specific DNA methylation by using exonuclease III (Exo III)-based recycling strategy (Fig. 5B) (Chen and Li, 2014). After the bisulfite treatment, the methylated DNA can hybridize with the fluorescein (FAM)-labeled probe (which is bound on the grapheme oxide) to form a double-stranded DNA (dsDNA), inducing the dissociation of FAM-labeled probes from the grapheme oxide and the recovery of FAM fluorescence and consequently the occurrence of CRET from luminol–H_2O_2–HRP to FAM. Notably, the Exo III-assisted recycling digestion of dsDNAs can induce significant signal amplification. This biosensor exhibits high sensitivity, and it can distinguish as low as 0.002% methylation level from the mixture, superior to most of currently reported DNA methylation assays.

3.4. Ligase chain reaction amplification

Ligase chain reaction (LCR) is a thermostable DNA ligase-dependent DNA amplification which can be initiated by repetitive cycles of the ligation of adjacent hybridized DNA probes for the achievement of exponential amplification of target DNA (Cao, 2004). Li et al. developed a size-coded LCR-based biosensor for simultaneous quantification of multiple miRNAs (Zhang et al., 2014). To improve the ligation efficiency, one of the DNA probes is modified with two ribonucleotides (defined as probe A-M). Target miRNA can adjacently hybridize with probe A-M and another probe, inducing the ligation between them and subsequently initiating LCR to produce a large amount of double-stranded DNA duplexes. The LCR products are separated by capillary electrophoresis (CE) under denaturing conditions and detected with laser induced fluorescence (LIF). Different kinds of target miRNAs can be simultaneously detected in one LCR reaction. This biosensor can quantify miRNA with a detection limit of 0.2 fM, and discriminate a single-nucleotide difference among miRNA sequences. Importantly, this biosensor possesses the multiplexing capability, and it can detect miRNAs of up to 50 different species.

By integrating LCR with AuNPs, Li et al. developed a colorimetric biosensor for the detection of CpG methylation in genomic DNA (Fig. 6A) (Su et al., 2015). After the treatment of genomic DNA with sodium bisulfite, the methylated cytosines (target M) remain unchanged, but the unmethylated cytosines (target N) are converted to uracils. Upon the addition of DNA ligase, probe A and probe B are joined to form DNA strand AB with target M as the ligation template. Similarly, probe A′ and probe B′ can form DNA strand A'B' with strand AB as the ligation template. Subsequently, the LCR products are exponentially amplified, with the unnecessary strands being digested by Exo III and I. Afterwards, the DNA strands immobilized on AuNPs can adjacently hybridize with the single-stranded A'B', inducing the network aggregation and generating a red-to-blue color change. This biosensor can be detected as low as 0.01 fM methylated DNA, and differentiate 0.1% methylated DNA in the presence of unmethylated DNA. Moreover, this biosensor can detect as low as 1 ng of methylated

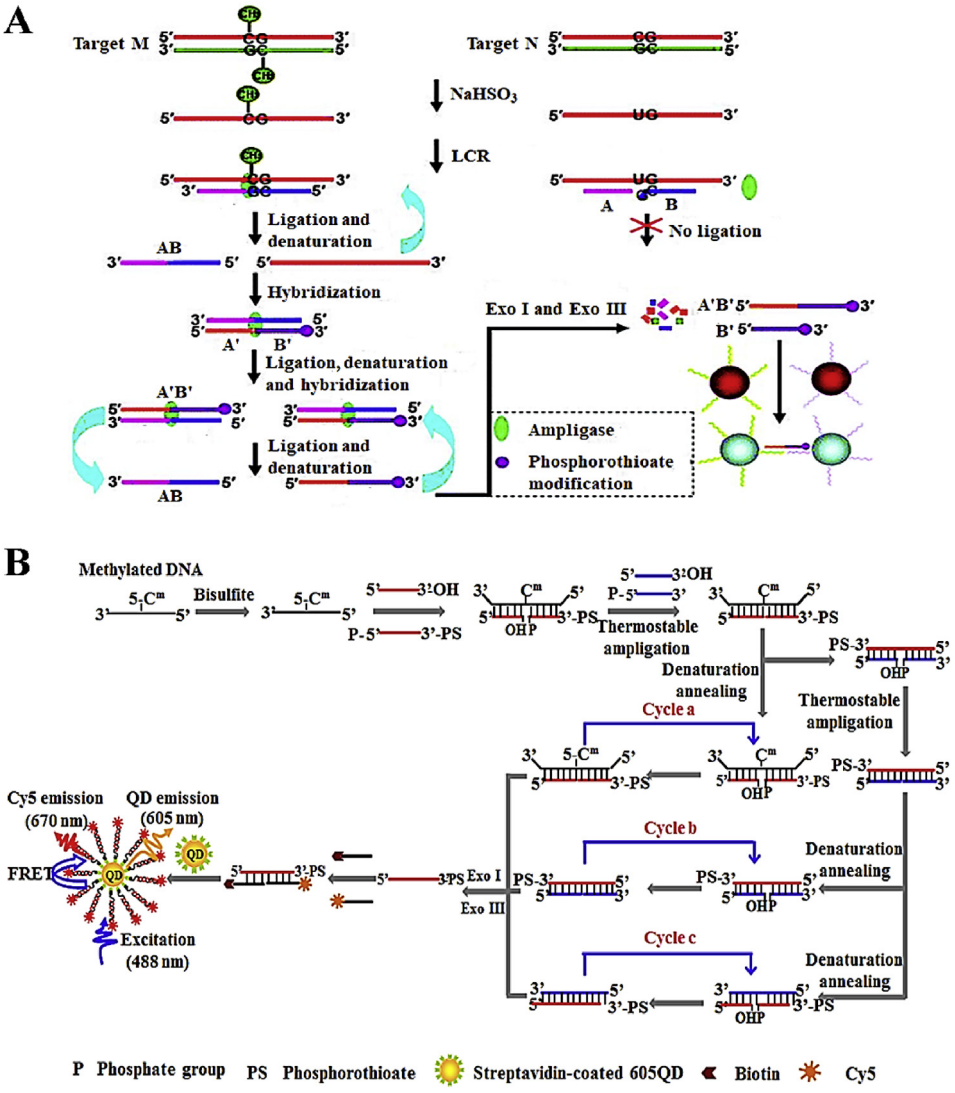

Fig. 6. Development of LCR-based biosensors for epigenetic inheritance assay. (A) Schematic illustration of colorimetric detection of CpG methylation. The presence of methylated DNA initiates the LCR whose products can subsequently induce the network aggregation of AuNPs to generate a color change. Reprinted from (Su et al., 2015) with the permission from the Royal Society of Chemistry. (B) Schematic illustration of fluorescent detection of DNA methylation based on smFRET and tricyclic LCR. In the presence of methylated DNA, tricyclic LCR is initiated, and the resultant products can subsequently hybridize with the biotinylated capture probes and the Cy5-labeled reporter probes to form the sandwich hybrids, inducing efficient FRET between the QD and Cy5. Reprinted from (Wang et al., 2018b) with the permission from the Royal Society of Chemistry. (For interpretation of the references to color in this figure legend, the reader is referred to the Web version of this article.)

genomic DNA extracted from whole blood of a healthy volunteer. In addition, Trau presented a biosensing platform for multiplexed detection of DNA methylation at CpG sites using SERS in combination with LCR (Wang et al., 2015). After treatment with bisulfite, target DNA is amplified by LCR reaction. The obtained products contain two specially designed sequences: one is a universal barcode sequence for capturing SERS array, and the other is a methylation state-specific barcode for SERS nanotag labeling. This biosensor exhibits a detection limit of 0.5 pM, and it can discriminate 10% difference in methylation. Moreover, this biosensor can be applied for real sample (e.g., serum-derived DNA sample and breast cancer cell lines) analysis.

To further enhance sensitivity, Zhang et al. took advantage of single-molecule Förster resonance energy transfer (smFRET) and tricyclic LCR (Walt, 2013) to develop a single quantum dot (QD)-based nanosensor for sensitive detection of DNA methylations at both CpG and nonCpG sites (Fig. 6B) (Wang et al., 2018b). After the treatment of target DNA with bisulfite, two sets of DNA probes (X and Y, X′ and Y′) are introduced to induce DNA methylation-actuated tricyclic LCR amplification, generating large amounts of XY products. The resultant XY products can hybridize with the biotinylated capture probes and the Cy5-labeled reporter probes to form the sandwich hybrids which can assemble on the QD surface to form the QD-oligonucleotide-Cy5 nanostructures, inducing efficient FRET between the QD and Cy5. This nanosensor can detect DNA methylation at both CpG and nonCpG sites with a detection limit of 1.0 aM and a large dynamic range of 7 orders of magnitude. Moreover, it can distinguish as low as a 0.01% methylation level, and further accurately measure the DNA methylation level even from 1 lung cancer cell.

3.5. Other amplification-based biosensors

Besides the above amplification approaches, the loop-mediated isothermal amplification (LAMP) (Tomita et al., 2008; Watanabe et al., 2000), hybridization chain reaction (HCR) (Venkataraman et al., 2007; Yin et al., 2008) and catalytic hairpin assembly (CHA) (Tao et al., 2015) have been introduced for the development of various biosensors for epigenetic biomarkers assays. LAMP is a nucleic acid amplification technique based on four or six primers-mediated autocycling strand displacement DNA synthesis, achieving $\sim 10^9$ copies accumulates from less than 10 copies of input template under isothermal condition within 1 h (Tomita et al., 2008; Watanabe et al., 2000). Li et al. reported a LAMP-based biosensor for the detection of site-specific DNA methylation (Fig. 7A) (Wen et al., 2016). After the treatment of DNA targets with methylation-sensitive restriction endonuclease, the methylated DNA remains intact. The methylated DNA can subsequently serve as the template to initiate the LAMP for real-time monitoring of DNA methylation with SYBR Green I as the fluorescent indicator. This biosensor can achieve a detection limit of as low as 10 aM, and it can discriminate 0.1% methylated DNA among a large excess of unmethylated DNA.

HCR is an enzyme-free amplification technique. In the presence of

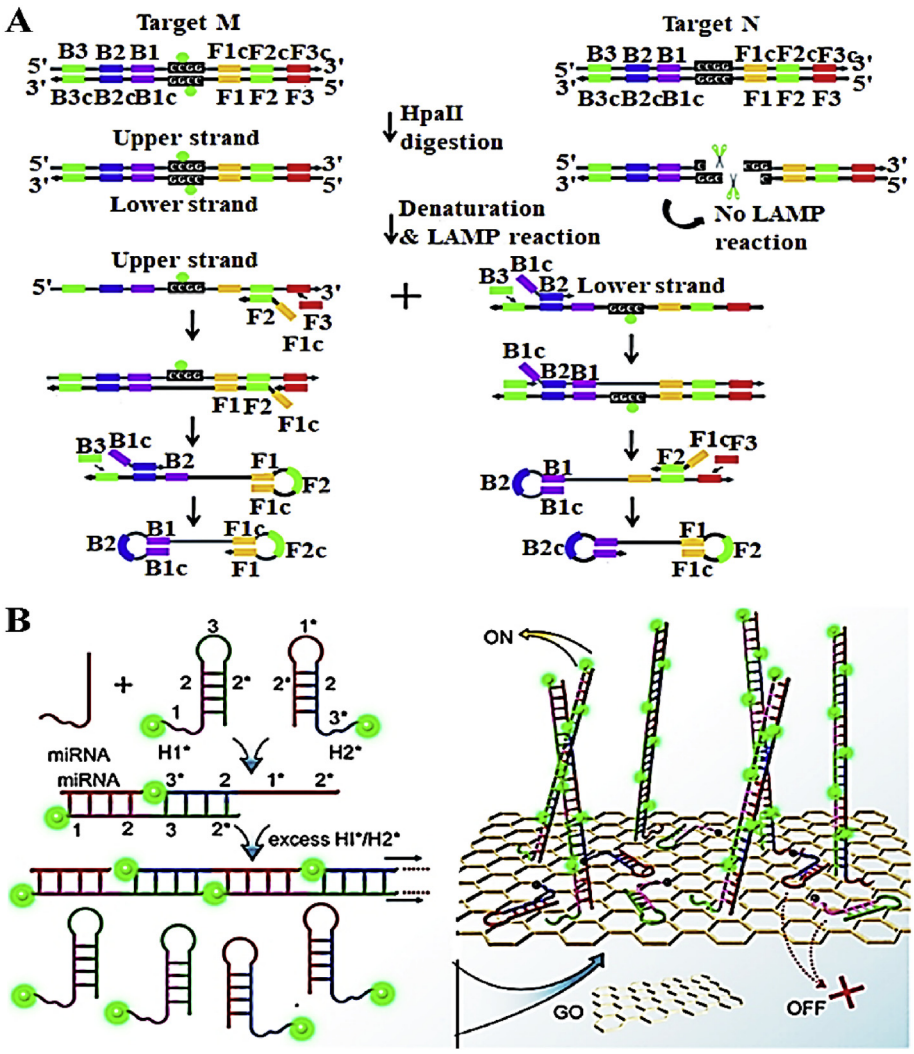

Fig. 7. Development of other biosensors for epigenetic inheritance assay. (A) Schematic illustration of LAMP-based biosensor for the detection of site-specific DNA methylation. Methylated DNA can serve as the template to initiate LAMP for real-time fluorescent monitoring of site-specific DNA methylation. Reprinted from (Wen et al., 2016) with the permission from the Royal Society of Chemistry. (B) Schematic illustration of fluorescent detection of miRNA based on the integration of HCR with GO. The presence of miRNA can initiate HCR between two species of fluorescent dye (FAM)-labeled hairpin probes. The fluorescence of the excess hairpin probes is completely quenched by GO, but the HCR products emit a strong fluorescence. Reprinted from (Yang et al., 2012) with the permission from the American Chemical Society.

target nucleic acid, it can initiate a cascade of hybridization events between two species of metastable hairpin probes to yield a nicked double-stranded DNA structure (Venkataraman et al., 2007). Yang et al. integrated HCR with graphene oxide (GO) to develop a fluorescent biosensor for miRNA detection (Fig. 7B) (Yang et al., 2012). The presence of target miRNA can initiate HCR between two species of fluorescent dye (FAM)-labeled hairpin probes (i.e., H1 and H2). Subsequently, the resultant HCR products and the excess hairpin probes are anchored on the GO surface. The fluorescence of the excess hairpin probes is completely quenched by GO, but the HCR products emit a strong fluorescence. The detection limit of this biosensor can reach 1 pM. Interestingly, the enriched fluorescence signals of the HCR products are dominantly gathered on the GO surface instead of in the solution, endowing the signal readout of HCR via fluorescence microscope or flow cytometer and holding great potential for in-situ fluorescence imaging or flow cytometry analysis of miRNAs.

CHA is also an enzyme-free amplification technique based on the accelerated hybridization between two DNA hairpin probes catalyzed by an input target (Tao et al., 2015). Liao et al. demonstrated a CHA-based electrochemiluminescent (ECL) biosensor for miRNA detection using two hairpin probe (i.e., H1 and H2) (Liao et al., 2014). In the presence of target miRNA, the stem of hairpin probe (H1) will be unfolded to expose the sequence hidden in H1 stem, which may subsequently unfold H2. The interaction of H1 with H2 induces the release of target miRNAs which can initiate the cyclic enzyme-free amplification for the generation of abundant H1–H2 complexes. The resultant H1–H2 complexes are captured by the streptavidin-conjugated magnetic beads to generate an ECL signal. This biosensor can detect 10, 10 and 100 copies of intracellular microRNAs in HepG2, A549, and breast adenocarcinoma (MCF-7 cells) cell lines, respectively, and it can achieve high detection accuracy for clinical tumor tissues analysis through increasing sample dosages and multidrawing tumor tissues.

4. Detection of other epigenetic biomarkers

Besides the above-mentioned epigenetic biomarkers (i.e., ncRNA, DNA methylation, and HEM), other epigenetic biomarkers including long noncoding RNA (lncRNA), 5-hydroxymethylcytosine (5-hmC) and SUMOylation can be accurately detected by a variety of biosensors. The lncRNA is a newly identified functional ncRNA with important regulatory roles in various pathophysiological processes (Gao et al., 2017). Liu et al. used the protein interaction data to obtain the expression profile of lncRNAs and protein-coding genes (PCGs), and built a lncRNA–PCG bipartite network. This biosensor may enable a large-scale prediction of cancer-related lncRNAs (Liu et al., 2015). Recently, Zhang et al. developed a fluorescent biosensor for the detection of lncRNAs on the basis of DSN-actuated cyclic enzymatic repairing-mediated signal amplification (Zhang et al., 2019). This biosensor can detect lncRNA with a detection limit of 0.081 fM and a large dynamic range of 9 orders of magnitude. Moreover, it can be applied to measure the endogenous lncRNA HOX transcript antisense RNA (HOTAIR) in different cancer cells (e.g., human bronchial epithelial cell line (HBE cells), A549 cells,

and HeLa cells).

The 5-hmC is proposed to be an intermediate in an active DNA demethylation pathway and a stable epigenetic modification which contributes unique regulatory functions to the epigenome (Cao et al., 2014). Chen et al. developed a multiplexing electrochemical biosensor to detect 5-hmC by integrating the glycosylation modification of 5-hmC with the enzymatic signal amplification (Chen et al., 2016). The 5-hmC can be detected at the subnanogram level (the detection limit is 0.489 pg). Moreover, benefited by its multiplexing capacity, this biosensor is time-saving and cost-effectiveness.

SUMOylation is a reversible post-translational modification by the small ubiquitin-like modifiers (SUMOs), and it plays critical roles in a variety of cellular processes (e.g., transcription, cellular localization, DNA repair and cell cycle progression) (Seeler and Dejean, 2003; Wilkinson and Henley, 2010). Zhang et al. demonstrated the simultaneous detection of intracellular SUMOylations at the single-molecule level by integrating SNAP/CLIP-tag-mediated translation with TIRF-based single-molecule imaging (Yang and Zhang, 2013). The detection limit of SUMOylated p53 proteins can reach as low as 5 pg. Importantly, taking advantage of the common translation module, the biosensor can be expanded to measure any ubiquitin-like modifications by genetic fusion of the ubiquitin-like modifiers with the SNAP/CLIP-tag.

5. Conclusions and perspectives

Epigenetics is one of the most rapidly expanding parts in the biological field, and the abnormal expression of epigenetic inheritance will affect chromatin structure and gene expression, leading to complex syndromes and cancers. Thus, the accurate monitoring of epigenetic biomarkers can help us prevent malicious epigenetic inheritance and evaluate the therapeutic efficacy. In this review, we summarize the recent development of biosensors for the epigenetic biomarkers assays, including the detection of ncRNA, DNA methylation, histone modification, and HEMs. These biosensors can be classified into two categories including the direct amplification-free and the nucleotide amplification-assisted biosensors. The direct biosensors have the advantages of simplicity and rapidity, but they always suffer from limited sensitivity and involve the expensive labels and the sophisticated instruments. Alternatively, the nucleotide amplification techniques such as PCR, SDA, EASA, LCR, LAMP, HCR and CHA have been introduced for epigenetic biomarkers assays. The nucleotide amplification-assisted biosensors exhibit high sensitivity, but the involvement of multiple enzymes might complicate the experimental procedures and increase the analysis time, limiting their wide practical applications.

Because of the extremely low abundance of epigenetic biomarkers in cells, it is a prospective direction to develop more sensitive biosensors for epigenetic biomarkers assays. The introduction of efficient amplification approaches, novel nanomaterials and new fluorescent labels may significantly improve the detection efficiency. Moreover, taking into account the fact that one disease is usually associated with multiple epigenetic biomarkers, the development of multiplexed biosensors for simultaneous detection of multiple epigenetic biomarkers is highly desirable. Especially, the monitoring of epigenetic biomarkers in vivo is still at the initial stage, and the recruition of some novel nanomaterials (e.g., AuNPs and QDs) has the potential to improve the performance of in vivo assays. Currently, most of the epigenetic biomarkers assays focus on miRNAs, DNA methylation and HEMs, and more efforts should be put into the development of new efficient biosensors for sensitive detection of other important epigenetic biomarkers such as lncRNA, 5-hmC, and SUMOylation. Due to its remarkable advantages of high signal-to-noise ratio, low sample consumption, and the improved sensitivity, the newly emerging single-molecule detection technique may become a promising future direction for the development of efficient epigenetic biomarkers biosensors. The introduction of single-molecule detection technique may greatly improve the sensitivity of epigenetic biomarkers biosensors even without the involvement of the complicated nucleotide amplification reactions. As the alternatives to organic dyes, semiconductor QDs possess distinct optical characteristics of good photochemical stability, high quantum yield, long fluorescence lifetime, broad spectral windows, narrow and size-tunable emission spectra. The QDs can be applied for the development of single QD-based biosensors, enabling simultaneous detection of multiple epigenetic biomarkers and multi-imaging of various epigenetic modifications in living organisms. We believe the development of new biosensors for epigenetic biomarkers assays may greatly facilitate our understanding the physiological function of epigenetic inheritance in human diseases and promote the epigenetic inheritance-related early clinical diagnosis and drug discovery.

CRediT authorship contribution statement

Chen-chen Li: Writing - original draft, Writing - review & editing. **Zi-yue Wang:** Writing - original draft, Writing - review & editing. **Li-juan Wang:** Writing - original draft, Writing - review & editing. **Chun-yang Zhang:** Writing - original draft, Writing - review & editing.

Declaration of Competing interest

The authors declare that they have no known competing financial interests or personal relationships that could have appeared to influence the work reported in this paper.

Acknowledgements

This work was supported by the National Natural Science Foundation of China (Grant Nos. 21735003, 21527811, and 21705097), and the Award for Team Leader Program of Taishan Scholars of Shandong Province, China.

References

Amaral, P.P., Dinger, M.E., Mercer, T.R., Mattick, J.S., 2008. Science 319, 1787–1789.
Bai, J., Zhao, Y., Wang, Z., Liu, C., Wang, Y., Li, Z., 2013. Anal. Chem. 85, 4813–4821.
Bhaumik, S.R., Smith, E., Shilatifard, A., 2007. Nat. Struct. Mol. Biol. 14, 1008–1016.
Bird, A., 2007. Nature 447, 396–398.
Bo, B., Zhang, T., Jiang, Y.T., Cui, H.Y., Miao, P., 2018. Anal. Chem. 90, 2395–2400.
Bonaldi, T., Regula, J.T., Imhof, A., 2004. Methods Enzymol. 377, 111–130.
Cao, A.P., Zhang, C.Y., 2012. Anal. Chem. 84, 6199–6205.
Cao, W., 2004. Trends Biotechnol. 22, 38–44.
Cao, Z., Zhou, N., Zhang, Y., Zhang, Y., Wu, R., Li, Y., Zhang, Y., Li, N., 2014. Theriogenology 81, 496–508.
Castaneda, A.D., Brenes, N.J., Kondajji, A., Crooks, R.M., 2017. J. Am. Chem. Soc. 139, 7657–7664.
Cenis, J.L., 1992. Nucleic Acids Res. 20 2380-2380.
Chen, C., Li, B.X., 2014. Biosens. Bioelectron. 54, 48–54.
Chen, F., Wang, X.Y., Cao, X.W., Zhao, Y.X., 2017. Anal. Chem. 89, 10468–10473.
Chen, S., Dou, Y., Zhao, Z., Li, F., Su, J., Fan, C., Song, S., 2016. Anal. Chem. 88, 3476–3480.
Deng, H.M., Ren, Y.Q., Shen, W., Gao, Z.Q., 2013. Chem. Commun. 49, 9401–9403.
Dong, H., Jin, S., Ju, H., Hao, K., Xu, L.-P., Lu, H., Zhang, X., 2012. Anal. Chem. 84, 8670–8674.
Egger, G., Liang, G., Aparicio, A., Jones, P.A., 2004. Nature 429, 457–463.
Esquela-Kerscher, A., Slack, F.J., 2006. Cancer 6, 259–269.
Friedlander, M.R., Lizano, E., Houben, A.J.S., Bezdan, D., Banez-Coronel, M., Kudla, G., Mateu-Huertas, E., Kagerbauer, B., Gonzalez, J., Chen, K.C., LeProust, E.M., Marti, E., Estivill, X., 2014. Genome Biol. 15, 17.
Gao, Y.-L., Zhao, Z.-S., Zhang, M.-Y., Han, L.-J., Dong, Y.-J., Xu, B., 2017. Oncol. Res. 25, 1391–1398.
Ge, C., Fang, Z., Chen, J., Liu, J., Lu, X., Zeng, L., 2012. Analyst 137, 2032–2035.
Ge, Z.L., Lin, M.H., Wang, P., Pei, H., Yan, J., Sho, J.Y., Huang, Q., He, D.N., Fan, C.H., Zuo, X.L., 2014. Anal. Chem. 86, 2124–2130.
Ghadiali, J.E., Lowe, S.B., Stevens, M.M., 2011. Angew. Chem. Int. Ed. 50, 3417–3420.
Gilboa, T., Torfstein, C., Juhasz, M., Grunwald, A., Ebenstein, Y., Weinhold, E., Meller, A., 2016. ACS Nano 10, 8861–8870.
Grant, P.A., Eberharter, A., John, S., Cook, R.G., Turner, B.M., Workman, J.L., 1999. J. Biol. Chem. 274, 5895–5900.
Hiraoka, D., Yoshida, W., Abe, K., Wakeda, H., Hata, K., Ikebukuro, K., 2012. Anal. Chem. 84, 8259–8264.
Horiuchi, K.Y., Eason, M.M., Ferry, J.J., Planck, J.L., Walsh, C.P., Smith, R.F., Howitz, K.T., Ma, H., 2013. Assay Drug Dev. Technol. 11, 227–236.
Hu, J., Liu, M.H., Zhang, C.Y., 2018. Chem. Sci. 9, 4258–4267.

Hu, Y.F., Chen, S.Y., Han, Y.T., Chen, H.J., Wang, Q., Nie, Z., Huang, Y., Yao, S.Z., 2015. Chem. Commun. 51, 17611–17614.
Huang, J., Zhang, S., Mo, F., Su, S., Chen, X., Li, Y., Fang, L., Huang, H., Deng, J., Liu, H., Yang, X., Zheng, J., 2019. Biosens. Bioelectron. 127, 155–160.
Hulshoff, M.S., Xu, X., Krenning, G., Zeisberg, E.M., 2018. Arterioscl. Throm. Vas. 38, 1986–1996.
Iwata, A., Nagata, K., Hatsuta, H., Takuma, H., Bundo, M., Iwamoto, K., Tamaoka, A., Murayama, S., Saido, T., Tsuji, S., 2014. Hum. Mol. Genet. 23, 648–656.
Jones, P.A., Baylin, S.B., 2002. Nat. Rev. Genet. 3, 415–428.
Labib, M., Sargent, E.H., Kelley, S.O., 2016. Chem. Rev. 116, 9001–9090.
Lagos-Quintana, M., Rauhut, R., Lendeckel, W., Tuschl, T., 2001. Science 294, 853–858.
Lee, J.-S., Han, M.S., Mirkin, C.A., 2007. Angew. Chem. Int. Ed. 46, 4093–4096.
Li, J.J., Liu, Q.Y., Xi, H.Y., Wei, X.C., Chen, Z.B., 2017a. Anal. Chem. 89, 12850–12856.
Li, K.K., Luo, C., Wang, D.X., Jiang, H.L., Zheng, Y.G., 2012. Med. Res. Rev. 32, 815–867.
Li, N.X., Du, M.Y., Liu, Y.C., Ji, X.H., He, Z.K., 2018. ACS Sens. 3, 1283–1290.
Li, R.D., Yin, B.C., Ye, B.C., 2016. Biosens. Bioelectron. 86, 1011–1016.
Li, S.C., Essaghir, A., Martijn, C., Lloyd, R.V., Demoulin, J.B., Oberg, K., Giandomenico, V., 2013. Mod. Pathol. 26, 685–696.
Li, X.M., Zhang, H.C., Tang, Y.R., Wu, P., Xu, S.X., Zhang, X.F., 2017b. ACS Sens. 2, 810–816.
Liao, H.X., Zhou, Y., Chai, Y.Q., Yuan, R., 2018. Biosens. Bioelectron. 114, 10–14.
Liao, Y., Huang, R., Ma, Z., Wu, Y., Zhou, X., Xing, D., 2014. Anal. Chem. 86, 4596–4604.
Lin, S., Gregory, R.I., 2015. Nat. Rev. Cancer 15, 321–333.
Lister, R., Pelizzola, M., Dowen, R.H., Hawkins, R.D., Hon, G., Tonti-Filippini, J., Nery, J.R., Lee, L., Ye, Z., Ngo, Q.-M., Edsall, L., Antosiewicz-Bourget, J., Stewart, R., Ruotti, V., Millar, A.H., Thomson, J.A., Ren, B., Ecker, J.R., 2009. Nature 462, 315–322.
Liu, Y., Wei, M., Li, Y., Liu, A., Wei, W., Zhang, Y., Liu, S., 2017. Anal. Chem. 89, 3430–3436.
Liu, Y., Zhang, R., Qiu, F., Li, K., Zhou, Y., Shang, D., Xu, Y., 2015. Mol. Biosyst. 11, 384–393.
Ma, F., Liu, M., Wang, Z.Y., Zhang, C.Y., 2016. Chem. Commun. 52, 1218–1221.
Medley, C.D., Smith, J.E., Tang, Z., Wu, Y., Bamrungsap, S., Tan, W., 2008. Anal. Chem. 80, 1067–1072.
Park, J., Yeo, J.S., 2014. Chem. Commun. 50, 1366–1368.
Portela, A., Esteller, M., 2010. Nat. Biotechnol. 28, 1057–1068.
Povedano, E., Valverde, A., Montiel, V.R.V., Pedrero, M., Yanez-Sedeno, P., Barderas, R., San Segundo-Acosta, P., Pelaez-Garcia, A., Mendiola, M., Hardisson, D., Campuzano, S., Pingarron, J.M., 2018. Angew. Chem. Int. Ed. 57, 8194–8198.
Prolo, C., Rios, N., Piacenza, L., Alvarez, M.N., Radi, R., 2018. Free Radic. Biol. Med. 128, 59–68.
Qu, W.S., Liu, Y.Y., Liu, D.B., Wang, Z., Jiang, X.Y., 2011. Angew. Chem. Int. Ed. 50, 3442–3445.
Roda, A., Pasini, P., Musiani, M., Girotti, S., Baraldini, M., Carrea, G., Suozzi, A., 1996. Anal. Chem. 68, 1073–1080.
Seeler, J.-S., Dejean, A., 2003. Nat. Rev. Mol. Cell Biol. 4, 690.
Sekar, T.V., Foygel, K., Gelovani, J.G., Paulmurugan, R., 2015. Anal. Chem. 87, 892–899.
Shen, Z.F., Li, F., Jiang, Y.F., Chen, C., Xu, H., Li, C.C., Yang, Z., Wu, Z.S., 2018. Anal. Chem. 90, 3335–3340.
Shi, Y.-J., Matson, C., Lan, F., Iwase, S., Baba, T., Shi, Y., 2005. Mol. Cell 19, 857–864.
Stains, C.I., Furman, J.L., Segal, D.J., Ghosh, I., 2006. J. Am. Chem. Soc. 128, 9761–9765.
Su, F.X., Wang, L.M., Sun, Y.Y., Liu, C.H., Duan, X.R., Li, Z.P., 2015. Chem. Commun. 51, 3371–3374.
Sun, Y.Y., Sun, Y.Y., Tian, W.M., Liu, C.H., Gao, K.J., Li, Z.P., 2018. Chem. Sci. 9, 1344–1351.
Tachibana, M., Sugimoto, K., Fukushima, T., Shinkai, Y., 2001. J. Biol. Chem. 276, 25309–25317.
Tang, X., Deng, R.J., Sun, Y.P., Ren, X.J., Zhou, M.X., Li, J.H., 2018. Anal. Chem. 90, 10001–10008.
Tao, C., Yan, Y., Xiang, H., Zhu, D., Cheng, W., Ju, H., Ding, S., 2015. Chem. Commun. 51, 4220–4222.
Thevenot, D.R., Toth, K., Durst, R.A., Wilson, G.S., 2001. Biosens. Bioelectron. 16, 121–131.
Tikhodeyev, O.N., 2018. Biol. Rev. 93, 1987–2005.
Tomita, N., Mori, Y., Kanda, H., Notomi, T., 2008. Nat. Protoc. 3, 877.
Tong, Q., Wang, W.J., Fan, Y.N., Dong, L., 2018. Trac. Trends Anal. Chem. 106, 246–258.
Van de Bittner, G.C., Dubikovskaya, E.A., Bertozzi, C.R., Chang, C.J., 2010. P. Natl. Acad. Sci. USA. 107, 21316–21321.
Van Ness, J., Van Ness, L.K., Galas, D.J., 2003. Proc. Natl. Acad. Sci. 100 (8), 4504–4509.
Venkataraman, S., Dirks, R.M., Rothemund, P.W.K., Winfree, E., Pierce, N.A., 2007. Nat. Nanotechnol. 2, 490.
Verma, M., Maruvada, P., Srivastava, S., 2004. Crit. Rev. Clin. Lab. Sci. 41 (5–6), 585–607.
Walt, D.R., 2013. Anal. Chem. 85, 1258–1263.
Wang, J., Xu, W.B., Yang, Z.C., Yan, Y.C., Xie, X.X., Qu, N., Wang, Y., Wang, C.Y., Hua, J.L., 2018a. ACS Appl. Mater. Interfaces 10, 31088–31095.
Wang, X., Huang, S.C., Huang, T.X., Su, H.S., Zhong, J.H., Zeng, Z.C., Li, M.H., Ren, B., 2017. Chem. Soc. Rev. 46, 4020–4041.
Wang, Y., Deng, X.H., Liu, J.W., Tang, H., Jiang, J.H., 2013. Chem. Commun. 49, 8489–8491.
Wang, Y.L., Wee, E.J.H., Trau, M., 2015. Chem. Commun. 51, 10953–10956.
Wang, Y.L., Wee, E.J.H., Trau, M., 2016. Chem. Commun. 52, 3560–3563.
Wang, Z.Y., Wang, L.J., Zhang, Q.Y., Tang, B., Zhang, C.Y., 2018b. Chem. Sci. 9, 1330–1338.
Watanabe, K., Masubuchi, H., Okayama, H., Amino, N., Hase, T., Yonekawa, T., Notomi, T., 2000. Nucleic Acids Res. 28 e63-e63.
Wen, H., Wang, H., Wang, H., Yan, J., Tian, H., Li, Z., 2016. Anal. Methods 8, 5372–5377.
Wen, Q., Gu, Y., Tang, L.J., Yu, R.Q., Jiang, J.H., 2013. Anal. Chem. 85, 11681–11685.
Wilkinson, Kevin A., Henley, Jeremy M., 2010. Biochem. J. 428, 133–145.
Wolffe, A.P., Matzke, M.A., 1999. Science 286, 481–486.
Wu, G., Jose, P.A., Zeng, C., 2018. Hypertension 72, 1047–1059.
Wynne Aherne, G., Rowlands, M.G., Stimson, L., Workman, P., 2002. Methods 26, 245–253.
Xu, W., Xue, X., Li, T., Zeng, H., Liu, X., 2009. Angew. Chem. Int. Ed. 48, 6849–6852.
Yanaihara, N., Caplen, N., Bowman, E., Seike, M., Kumamoto, K., Yi, M., Stephens, R.M., Okamoto, A., Yokota, J., Tanaka, T., Calin, G.A., Liu, C.-G., Croce, C.M., Harris, C.C., 2006. Cancer Cell 9, 189–198.
Yang, L., Liu, C., Ren, W., Li, Z., 2012. ACS Appl. Mater. Interfaces 4, 6450–6453.
Yang, Y., Zhang, C.-y., 2013. Angew. Chem. Int. Ed. 52, 691–694.
Ye, L.P., Hu, J., Liang, L., Zhang, C.Y., 2014. Chem. Commun. 50, 11883–11886.
Yin, P., Choi, H.M.T., Calvert, C.R., Pierce, N.A., 2008. Nature 451, 318.
Yoshida, W., Baba, Y., Karube, I., 2016. Anal. Chem. 88, 9264–9268.
Yoshida, W., Kezuka, A., Abe, K., Wakeda, H., Nakabayashi, K., Hata, K., Ikebukuro, K., 2013. Anal. Chem. 85, 6485–6490.
Yu, X.Z., Wen, K., Wang, Z.H., Zhang, X.Y., Li, C.L., Zhang, S.X., Shen, J.Z., 2016. Anal. Chem. 88, 3512–3520.
Zhang, P., Zhang, J., Wang, C., Liu, C., Wang, H., Li, Z., 2014. Anal. Chem. 86, 1076–1082.
Zhang, Y., Wang, X.-y., Su, X., Zhang, C.-y., 2019. Chem. Commun. 55, 6827–6830.
Zhang, Y., Zhang, C.Y., 2012. Anal. Chem. 84, 224–231.
Zhen, Z., Tang, L.J., Long, H.X., Jiang, J.H., 2012. Anal. Chem. 84, 3614–3620.
Zhou, D., Lin, X., Gao, W., Piao, J., Li, S., He, N., Qian, Z., Zhao, M., Gong, X., 2019. Chem. Commun. 55, 2932–2935.
Zhou, W., Tian, Y.F., Yin, B.C., Ye, B.C., 2017. Anal. Chem. 89, 6121–6129.
Zhu, G.C., Liang, L., Zhang, C.Y., 2014. Anal. Chem. 86, 11410–11416.
Zou, F., Ruan, Q., Lin, X., Zhang, M., Song, Y., Zhou, L., Zhu, Z., Lin, S., Wang, W., Yang, C.J., 2019. Biosens. Bioelectron. 126, 551–557.